Journal of Computational Physics **149,** 270–292 (1999)
Article ID jcph.1998.6153, available online at http://www.idealibrary.com on IDEAL®

A Staggered Mesh Algorithm Using High Order Godunov Fluxes to Ensure Solenoidal Magnetic Fields in Magnetohydrodynamic Simulations

Dinshaw S. Balsara* and Daniel S. Spicer†

*NCSA, University of Illinois at Urbana Champaign, Urbana, Illinois 61801; and †NCCS, Code 930, NASA/Goddard Space Flight Center, Greenbelt, Maryland 20771
E-mail: *dbalsara@ncsa.uiuc.edu and †spicer@gauss.gsfc.nasa.gov

Received January 8, 1998; revised September 21, 1998

The equations of magnetohydrodynamics (MHD) have been formulated as a hyperbolic system of conservation laws. In that form it becomes possible to use higher order Godunov schemes for their solution. This results in a robust and accurate solution strategy. However, the magnetic field also satisfies a constraint that requires its divergence to be zero at all times. This is a property that cannot be guaranteed in the zone centered discretizations that are favored in Godunov schemes without involving a divergence cleaning step. In this paper we present a staggered mesh strategy which directly uses the properly upwinded fluxes that are provided by a Godunov scheme. The process of directly using the upwinded fluxes relies on a duality that exists between the fluxes obtained from a higher order Godunov scheme and the electric fields in a plasma. By exploiting this duality we have been able to construct a higher order Godunov scheme that ensures that the magnetic field remains divergence-free up to the computer's round-off error. We have even presented a variant of the basic algorithm that uses multidimensional features in the flow to design an upwinded strategy that aligns itself with the predominant upwinded direction in the flow. We have devised several stringent test problems to show that the scheme works robustly and accurately in all situations. In doing so we have shown that a scheme that involves a collocation of magnetic field variables that is different from the one traditionally favored in the design of higher order Godunov schemes can nevertheless offer the same robust and accurate performance of higher order Godunov schemes provided the properly upwinded fluxes from the Godunov methodology are used in the scheme's construction.

1. INTRODUCTION

The requirement that solutions to the equations of magnetohydrodynamics (MHD) satisfy $\nabla \cdot \mathbf{B} = 0$ represents a severe constraint on any numerical scheme, as detailed by the work

0021-9991/99 $30.00

of Brackbill and Barnes [1, 2], where **B** is the magnetic field. This constraint manifests itself in two major ways. First, it represents a constraint on the topological properties of the magnetic field lines and its violation becomes acutely obvious when one is modelling phenomena associated with reconnection, something not safely ignored in laboratory, space, or astrophysical magnetized plasmas. The topological linkages of the magnetic lines are manifested through the global conservation of magnetic helicity

$$\mathcal{H} = \int \mathbf{A} \cdot \mathbf{B}\, d^3x, \tag{1}$$

where **A** is the magnetic vector potential. Not guaranteeing $\nabla \cdot \mathbf{B} = 0$ to round-off can radically alter one's physical interpretation of the role of global magnetic helicity as well as affect other globally conserved quantities. Further, numerically incorrect magnetic field topologies lead to unphysical plasma transport orthogonal to the magnetic field; see Brackbill and Barnes [1]. Second, violating the $\nabla \cdot \mathbf{B} = 0$ constraint results in loss of momentum and energy conservation, as well as allows fictitious forces to develop parallel to the magnetic field. For these reasons researchers have developed the so-called "staggered mesh magnetic field transport algorithm" which is based on the use of Stokes' theorem. This algorithm was first proposed by Yee [3] for the transport of electromagnetic fields. Later Brecht *et al.* [4] combined the staggered mesh approach with a non-linear FCT flux limiter to ensure that there were no non-physical under- and over-shoots in the magnetic fields in their global MHD modelling of Earth's magnetosphere. Evans and Hawley [5] then applied the hybrid scheme utilized by Brecht *et al.* [4] to an artificial viscosity based scheme, coining the term "constrained transport." Contemporaneously with Hawley and Evans [5], Devore [6] applied the same constrained transport scheme to a flux corrected transport (FCT) algorithm. Stone and Norman [7] made a variant of the scheme of Hawley and Evans [5], in which they used a method of characteristics approach to treat Alfvén waves.

There has been considerable recent interest in the construction of higher order Godunov schemes for MHD. A brief list of publications on this topic includes Zachary, Malagoli, and Colella [8], Dai and Woodward [9], Ryu and Jones [10], Roe and Balsara [11], and Balsara [12, 13]. All of these practitioners have shown at least some awareness of the fact that higher order Godunov schemes do not preserve the divergence-free aspect of the magnetic field. Not keeping the magnetic field divergence-free can cause an extra compressive component to arise in the magnetic field due to discretization errors that build up over time in the numerical problem. In higher order Godunov schemes one evolves the total energy. The pressure is obtained from subtracting the kinetic energy and the magnetic energy from the total energy. Thus if the magnetic field develops an extra, unphysical, compressive component then that reduces the gas pressure in the simulation. That fact, along with the fact that one of the eigenvalues of the MHD system is zero, prompted Powell [14] to modify the MHD equations by adding extra terms to the physical equations. Other practitioners in this field have not seen the value of modifying the physical equations themselves. Instead they have seen the value of divergence cleaning that essentially removes the compressive portion of the magnetic field. Balsara [12, 13] has in fact constructed certain detailed algorithms that go beyond the simple Hodge projection to ensure that the magnetic fields are divergence-free. Balsara [12, 13] also showed that allowing the magnetic fields to develop a compressive component in the course of a calculation can almost always be shown to produce some small errors in the solution. Thus over several time steps, the errors in the evaluation of the magnetic field can develop a substantial compressive and, therefore, unphysical component in the

magnetic field and thereby change the nature of the solution. Several divergence cleaning algorithms are fast and efficient and also very parallelizable if the right strategies such as multigrid methods or FETs are used to solve the resultant elliptic equations. However, the strategies mentioned above are not always adaptable to the use of different types of boundary conditions or different types of zoning. As a result we have developed the scheme that is presented in this paper.

In this paper we describe an algorithm that utilizes a staggered collocation of the solenoidal field components and utilizes higher order Godunov fluxes for their update. We demonstrate the technique for a dimensionally split higher order Godunov scheme for doing numerical MHD; however, there is nothing in the method that would prevent it from being utilized in a multi-stage scheme. It is also interesting to point out that the equations of incompressible flow also require the velocity field to be divergence-free. Higher order Godunov schemes for the incompressible Euler equations have been constructed; see E and Shu [16] and Bell, Colella, and Glaz [17]. Such schemes have so far relied on using the Hodge projection operator to make the velocity field solenoidal. Such schemes might also benefit from the very general strategy developed here. The method presented here directly uses the upwinded fluxes that are computed at the zone faces in higher order Godunov schemes. As a result, it is applicable in a general way to all situations where a solenoidal vector field needs to be updated. It does not depend on dimensional sweeping of the underlying higher order Godunov scheme and can accommodate higher order Godunov schemes that are multidimensional in the style of vanLeer [18] and Colella [19]. It works for predictor–corrector time–update strategies and also for multi-stage strategies. The method presented here relies on a conceptual interpretation of magnetic fields as area-weighted variables collocated at the centers of zone faces. It can, therefore, be trivially extended to essentially non-oscillatory (ENO) schemes of finite difference type (Shu and Osher [20]) and to ENO schemes of finite volume type (Harten *et al.* [21], Casper and Atkins [22]). We show through an extensive set of examples that the strategy presented in this paper offers robust handling of strong multidimensional shocks. As a result the concerns usually associated with staggered collocation of data in a numerical scheme have, therefore, been ameliorated.

It has been pointed out to us by a referee that Dai and Woodward [15] have also recently used a staggered collocation of field components. Their method does not use the upwinded fluxes. Instead it updates the field variables by using the zone averages and interpolates them to the zone edges in order to construct electric field components at the zone edges in the same way as Evans and Hawley [5]. However, Stone and Norman [7] found that the method of Evans and Hawley [5] was inadequate for the treatment of Alfvén wave propagation in two dimensional problems. The solution offered by Stone and Norman [7] was to abstract a 2×2 hyperbolic subsystem from the equations of MHD which they could solve for the propagation of Alfvén waves and apply a characteristics-based method to that hyperbolic subsystem in order to evaluate the electric fields. Thus the essential difference between the method of Stone and Norman [7] and the method of Evans and Hawley [5] was that the former authors directly used the upwinded variables to construct the electric fields while the latter authors used centered variables to do the same. The method of Stone and Norman [7] proves to be unsatisfying from a conceptual standpoint because not every MHD flow needs to be resolved as the propagation of Alfvén waves. It is also unreasonable to split a hyperbolic system into a subsystem just because one could solve that subsystem. Dai and Woodward [15] do not give several test problems where the dynamics is strongly governed by the propagation of Alfvén waves. It is, therefore, unclear whether their utilization of the

strategy of Evans and Hawley [5] for the evaluation of the electric fields suffers from the same problems as the ones pointed out by Stone and Norman [7]. It is possible that Dai and Woodward's use of the higher order Godunov methodology might have saved their method from having the worst deficiencies of the scheme of Evans and Hawley [5]. We, however, argue in this paper that the dualism between the the electric fields and the fluxes from the higher order Godunov scheme makes it unnecessary to update the electric fields in the same way as Evans and Hawley [5] and Dai and Woodward [15]. The higher order Godunov fluxes available from higher order Godunov schemes are in fact the properly upwinded variables that one should directly use in constructing the electric fields. We also show in Subsection 2.2 that this dual viewpoint allows us to formulate a scheme that is upwinded in a multidimensional sense. Thus there is a conceptual as well as an algorithmic advantage in the viewpoint adopted in this paper.

In Section 2 we describe the numerical methodology. We present the basic algorithm in Subsection 2.1 and a variant of the basic algorithm that uses multidimensional upwinding in regions with shocks in Subsection 2.2. In Section 3 we show some representative results. In Section 4 we draw some conclusions.

2. NUMERICAL METHODOLOGY

2.1. *The Basic Algorithm*

Our algorithm is based on the fact that there is a duality between the electric field and the fluxes produced by higher order Godunov schemes. Faraday's equation is given by

$$\frac{\partial \mathbf{B}}{\partial t} + \nabla \times \mathbf{E} = 0. \tag{2}$$

For ideal MHD the electric field $\mathbf{E}$ is given by

$$\mathbf{E} = -\mathbf{v} \times \mathbf{B} \tag{3}$$

though in other situations a more general Ohm's law may be used. The magnetic permeability is set to unity. Since our target applications are drawn from space physics and astrophysics this is a very good approximation for the magnetic permeability. As shown by Yee [3], Brecht *et al.* [4], Hawley and Evans [5], and DeVore [6] the above equations suggest that a discrete version of Stokes' theorem be used for the temporal update of the magnetic fields. In this interpretation, the three components of the magnetic field are collocated at the centers of the zone faces to which they are orthogonal. As a result the different components of the magnetic field are collocated at different spatial points in the control volume. The magnetic field is to be treated as an area-weighted average on the zone face. This area-weighted average is a strict analogue of the volume-weighted averages of fluid densities in fluid mechanics. The electric fields are collocated at zone edges. Then the line integral of the electric field over a zone edge gives the electromotive force (EMF) over that edge. Stokes' theorem in its discrete form consists of saying that the change in the magnetic flux associated with a zone face in the course of a time step is just the line integral of the electric field over the edges times the time step. In other words, this change is the sum of the EMFs over the zone edges bounding that zone face. Figure 1 shows the collocation of magnetic and electric field variables in a pictorial fashion. The discrete representation of Stokes' theorem will be explicitly written out in the context of the numerical scheme presented later in this section.

The above equations along with the equations for fluid mass, momentum, and energy conservation can be cast into conservative form. This is the form usually used in the

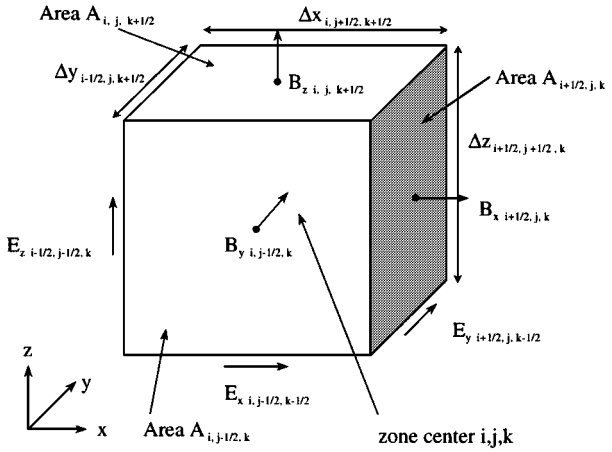

FIG. 1. The collocation of the magnetic fields as the control volume's faces and the collocation of the electric fields at the control volume's edges. The notation used in the paper is established.

construction of higher order Godunov schemes. In component form the full set of equations is given by

$$
\frac{\partial}{\partial t}\begin{pmatrix} \rho \\ \rho v_x \\ \rho v_y \\ \rho v_z \\ \mathcal{E} \\ B_x \\ B_y \\ B_z \end{pmatrix}
+ \frac{\partial}{\partial x}\begin{pmatrix} \rho v_x \\ \rho v_x^2 + P + B^2/8\pi - B_x^2/4\pi \\ \rho v_x v_y - B_x B_y/4\pi \\ \rho v_x v_z - B_x B_z/4\pi \\ (\mathcal{E} + P + \mathbf{B}^2/8\pi) v_x - B_x(\mathbf{v}\cdot\mathbf{B})/4\pi \\ 0 \\ -E_z \\ E_y \end{pmatrix}
$$

$$
+ \frac{\partial}{\partial y}\begin{pmatrix} \rho v_y \\ \rho v_x v_y - B_x B_y/4\pi \\ \rho v_y^2 + P + B^2/8\pi - B_y^2/4\pi \\ \rho v_y v_z - B_y B_z/4\pi \\ (\mathcal{E} + P + \mathbf{B}^2/8\pi) v_y - B_y(\mathbf{v}\cdot\mathbf{B})/4\pi \\ E_z \\ 0 \\ -E_x \end{pmatrix}
$$

$$
+ \frac{\partial}{\partial z}\begin{pmatrix} \rho v_z \\ \rho v_x v_z - B_z B_x/4\pi \\ \rho v_y v_z - B_z B_y/4\pi \\ \rho v_z^2 + P + B^2/8\pi - B_z^2/4\pi \\ (\mathcal{E} + P + \mathbf{B}^2/8\pi) v_z - B_z(\mathbf{v}\cdot\mathbf{B})/4\pi \\ -E_y \\ E_x \\ 0 \end{pmatrix} = 0 \qquad (4)
$$

or

$$\frac{\partial \mathbf{U}}{\partial t} + \frac{\partial \mathbf{F}}{\partial x} + \frac{\partial \mathbf{G}}{\partial y} + \frac{\partial \mathbf{H}}{\partial z} = 0, \tag{5}$$

where $\mathcal{E} = \rho \mathbf{v}^2/2 + P/(\gamma - 1) + \mathbf{B}^2/8\pi$. One finds the following symmetries with respect to the flux components:

$$F_7 = -G_6, \quad F_8 = -H_6, \quad G_8 = -H_7. \tag{6}$$

In a higher order Godunov scheme that is spatially and temporally second order accurate, these flux variables are available at the center of each zone's face using a straightforward Godunov approach. Moreover, these fluxes are spatially second order accurate and temporally centered. We want to work directly from these fluxes. The constrained flux approach utilizes the electric fields on the edges of the control volume in order to update the magnetic fields at the centers of the control volume's faces. The last three components of **F**, **G**, and **H** are just the higher order Godunov fluxes that are available at the control volume's face centers. In our dual interpretation of Godunov fluxes they alternatively represent electric fields on the faces, albeit with signs that might need to be changed. Thus we need to use the face centered, upwinded fluxes from the Godunov scheme in order to reconstruct electric fields on the edges of the control volume.

We make the discussion above more concrete with an example. At the edge center $(i + 1/2,\ j, k + 1/2)$ the electric field $E_y = -(v_z B_x - v_x B_z)$ scales as F_8, the eighth component of the x-directional Godunov flux. It also scales as $-H_6$, the sixth component of the z-directional Godunov flux. Of course, these upwinded fluxes are not available at the edge center but they are available as properly upwinded, time centered fluxes (that is, at time $t^{n+1/2}$, where $\Delta t = t^{n+1} - t^n$) at the face centers. More precisely, a spatially second order accurate version of F_8 is available during the x-sweep at positions $(i + 1/2,\ j, k)$ and $(i + 1/2,\ j, k + 1)$. Similarly, during a y-sweep, a spatially second order accurate version of $-H_6$ is available at positions $(i,\ j, k+1/2)$ and $(i+1,\ j, k+1/2)$. We can use the fluxes at these four locations to make a reconstruction of E_y at $(i + 1/2,\ j, k + 1/2)$ with second order accuracy in space and time. Thus we have

$$E^{n+1/2}_{x,\,i,\,j+1/2,k+1/2} = \frac{1}{4}\begin{pmatrix} H^{n+1/2}_{7,\,i,\,j,k+1/2} + H^{n+1/2}_{7,\,i,\,j+1,k+1/2} \\ -G^{n+1/2}_{8,\,i,\,j+1/2,k} - G^{n+1/2}_{8,\,i,\,j+1/2,k+1} \end{pmatrix} \tag{7}$$

$$E^{n+1/2}_{y,\,i+1/2,\,j,k+1/2} = \frac{1}{4}\begin{pmatrix} F^{n+1/2}_{8,\,i+1/2,\,j,k} + F^{n+1/2}_{8,\,i+1/2,\,j,k+1} \\ -H^{n+1/2}_{6,\,i,\,j,k+1/2} - H^{n+1/2}_{6,\,i+1,\,j,k+1/2} \end{pmatrix} \tag{8}$$

$$E^{n+1/2}_{z,\,i+1/2,\,j+1/2,k} = \frac{1}{4}\begin{pmatrix} G^{n+1/2}_{6,\,i,\,j+1/2,k} + G^{n+1/2}_{6,\,i+1,\,j+1/2,k} \\ -F^{n+1/2}_{7,\,i+1/2,\,j,k} - F^{n+1/2}_{7,\,i+1/2,\,j+1,k} \end{pmatrix}. \tag{9}$$

It might be useful to point out that the right hand sides of the above three equations are just an arithmetic sum of four terms and should not be confused with a matrix expression. The above equations apply to a grid with uniform zoning in each direction. Should the grid have spatially varying zone sizes, the linear reconstruction in the three equations above would

have to reflect the spatially varying zone size. Thus a perspective that emerges from the above three equations is that the averaging should be viewed as a reconstruction step. It might seem unusual to the reader who is only accustomed to second order schemes that flux components evaluated at four different points are combined in each of the above three equations. However, we point out the work of Casper and Atkins [22], where it was shown that the combination of fluxes that were evaluated at several points along each zone boundary is an essential step in the design of certain types of higher order Godunov schemes that seek to have better than second order accuracy. The staggering of variables along with the need to achieve second order accuracy creates a similar need to combine flux components that are evaluated at different points. It is also worthwhile to point out that the above three equations provide the most compact second order accurate representation of the electric fields that can be obtained at the zone edges. It must also be noted that the electric field is not a quantity that we evolve in time. As a result, the interpolation of flux components, which have a dual role as electric field components, in the above three equations does not introduce any significant level of numerical diffusion in the time evolution of the magnetic field. If we are using a multi-stage scheme where each stage in the scheme is only first order accurate in time (see Shu and Osher [20]), then the above equations should be applied to each fractional time level in the multi-stage scheme.

We first write out the time-update strategy for a dimensionally swept scheme which uses a predictor–corrector strategy to obtain spatially and temporally second order accurate updates of the field variables. Such a scheme has been catalogued in Balsara [12, 13]. With the result in the previous paragraph, it becomes obvious that we can accumulate the electric fields at the edge centers as we go through the dimensional sweeps. This allows us to write out the steps in the multidimensional scheme as follows:

(1) At the beginning of the time step start with mass, momenta, and energy at control volume centers and **B** at the appropriate face centers. Interpolate the magnetic field to the control volume centers. Because we construct a second order accurate scheme, second order accurate interpolation is adequate. Denote the vector of eight variables at the control volume centers as $\mathbf{U}^n_{i,j,k}$.

(2) Make an x-sweep to get fluxes **F** at the $x =$ constant faces. Make the usual update of the vector $\mathbf{U}^n_{i,j,k}$ at the control volume centers, that is,

$$\tilde{\mathbf{U}}^{n+1}_{i,j,k} = \mathbf{U}^n_{i,j,k} - \frac{\Delta t}{\Delta x}\left(F^{n+1/2}_{i+1/2,j,k} - F^{n+1/2}_{i-1/2,j,k}\right). \tag{10}$$

Also in this step, add in contributions of **F** to E_y using Eq. (8) and contributions of **F** to E_z using Eq. (9).

(3) Make a y-sweep to get fluxes **G** at $y =$ constant faces. Make the update

$$\tilde{\tilde{\mathbf{U}}}^{n+1}_{i,j,k} = \tilde{\mathbf{U}}^{n+1}_{i,j,k} - \frac{\Delta t}{\Delta y}\left(G^{n+1/2}_{i,j+1/2,k} - G^{n+1/2}_{i,j-1/2,k}\right). \tag{11}$$

Also in this step, add in contributions of **G** to E_x using Eq. (7) and contributions of **G** to E_z using Eq. (9).

(4) Make a z-sweep to get fluxes **H** at $z =$ constant faces. Make the update

$$\mathbf{U}^{n+1}_{i,j,k} = \tilde{\tilde{\mathbf{U}}}^{n+1}_{i,j,k} - \frac{\Delta t}{\Delta z}\left(H^{n+1/2}_{i,j,k+1/2} - H^{n+1/2}_{i,j,k-1/2}\right). \tag{12}$$

Also in this step, add in contributions of $\mathbf{H}$ to E_y using Eq. (8) and contributions of $\mathbf{H}$ to E_x using Eq. (7). At this point the first five components of $\mathbf{U}^{n+1}_{i,j,k}$ already contain the mass, momenta, and energy at time t^{n+1}. The last three components of $\mathbf{U}^{n+1}_{i,j,k}$ contain the zone centered representation of the magnetic fields given by straightforward application of the higher order Godunov scheme. Furthermore, the electric fields at all the edge centers contain all the contributions from the fluxes that they need to contain.

(5) Up to this point only the magnetic field components at the control volume centers have been changed but not the face centered values. However, since we now have all the edge centered components of the electric field we can now update all the components of the face centered magnetic fields. This is done by using a discrete version of Stokes' theorem as applied to Eq. (2) at each of the control volume's faces. Using the notation shown in Fig. 1 the discrete update equations for the face centered magnetic fields are given by

$$B^{n+1}_{x,\,i+1/2,\,j,k} = B^{n}_{x,\,i+1/2,\,j,k} - \frac{\Delta t}{A_{i+1/2,\,j,k}} \begin{pmatrix} \Delta z_{i+1/2,\,j+1/2,k} E^{n+1/2}_{z,\,i+1/2,\,j+1/2,k} \\ -\Delta z_{i+1/2,\,j-1/2,k} E^{n+1/2}_{z,\,i+1/2,\,j-1/2,k} \\ +\Delta y_{i+1/2,\,j,k-1/2} E^{n+1/2}_{y,\,i+1/2,\,j,k-1/2} \\ -\Delta y_{i+1/2,\,j,k+1/2} E^{n+1/2}_{y,\,i+1/2,\,j,k+1/2} \end{pmatrix} \tag{13}$$

$$B^{n+1}_{y,\,i,\,j-1/2,k} = B^{n}_{y,\,i,\,j-1/2,k} - \frac{\Delta t}{A_{i,\,j-1/2,k}} \begin{pmatrix} \Delta x_{i,\,j-1/2,k+1/2} E^{n+1/2}_{x,\,i,\,j-1/2,k+1/2} \\ -\Delta x_{i,\,j-1/2,k-1/2} E^{n+1/2}_{x,\,i,\,j-1/2,k-1/2} \\ +\Delta z_{i-1/2,\,j-1/2,k} E^{n+1/2}_{z,\,i-1/2,\,j-1/2,k} \\ -\Delta z_{i+1/2,\,j-1/2,k} E^{n+1/2}_{z,\,i+1/2,\,j-1/2,k} \end{pmatrix} \tag{14}$$

$$B^{n+1}_{z,\,i,\,j,k+1/2} = B^{n}_{z,\,i,\,j,k+1/2} - \frac{\Delta t}{A_{i,\,j,k+1/2}} \begin{pmatrix} \Delta x_{i,\,j-1/2,k+1/2} E^{n+1/2}_{x,\,i,\,j-1/2,k+1/2} \\ -\Delta x_{i,\,j+1/2,k+1/2} E^{n+1/2}_{x,\,i,\,j+1/2,k+1/2} \\ +\Delta y_{i+1/2,\,j,k+1/2} E^{n+1/2}_{y,\,i+1/2,\,j,k+1/2} \\ -\Delta y_{i-1/2,\,j,k+1/2} E^{n+1/2}_{y,\,i-1/2,\,j,k+1/2} \end{pmatrix}. \tag{15}$$

As before, it might be useful to point out that the right hand sides of the above three equations are just an arithmetic sum of four terms and should not be confused with a matrix expression.

(6) At this stage we have two sets of magnetic fields. One set of magnetic fields is collocated at the zone centers. The other set of magnetic fields is collocated at the zone faces that correspond to them. The interpolation of the face centered magnetic fields to the zone centers will in general differ slightly from the zone centered magnetic fields themselves. Although this difference is of the order of magnitude of the discretization error of the scheme, for low β plasmas this difference can be substantial enough to cause the pressure to become negative if it is not corrected for. Thus the magnetic fields stored on the faces are averaged to the zone center. They are then used to correct the energy density for the new magnetic field. That is, if $\mathbf{B}^{n+1}_{c}$ is the zone centered value of the magnetic field obtained by advancing the field directly using the high order Godunov scheme and $\mathbf{B}^{n+1}_{fc}$ is the new zone centered value of the magnetic field obtained by averaging the face centered values of the magnetic field to the zone center, then the energy density becomes

$$\mathcal{E} = \mathcal{E} + \left[\left(\mathbf{B}^{n+1}_{fc}\right)^2 - \left(\mathbf{B}^{n+1}_{c}\right)^2\right]/8\pi. \tag{16}$$

We point out that this step is an optional step. It results in a slight loss of total energy conservation at the level of discretization error. Several real world applications and several test problems have been run without this step and we did not encounter any problem associated with the evolution of the pressure variable. However, in problems involving very low β plasmas the positivity of the pressure variable is important for maintaining physical consistency. In such situations the present step, which is motivated by the need to maintain physical consistency, proves to be very useful.

In Balsara [12, 13], a multidimensional update strategy for evolving the MHD equations was also constructed. For such a scheme, the fluxes in the three dimensions in steps (2), (3), and (4) are available simultaneously. Thus the accumulation of upwinded fluxes to build up the electric fields at the zone edges can be done all at once. Thus the only difference when using the methods developed in this paper in multidimensional schemes is that steps (2), (3), and (4) above should be collapsed into a single step.

For schemes that produce fluxes that have spatial accuracy that is higher than second order the reconstruction step in Eqs. (7), (8), and (9) will have to be modified. Equations (13), (14), and (15) should remain valid for schemes that use finite difference discretizations that have higher than second order accuracy. For schemes that use finite volume discretizations to obtain higher than second order accuracy one will have to use the Simpson rule at a multiplicity of knots to perform the line integral of the electric fields. For such schemes Eqs. (13), (14), and (15) will also have to be suitably extended. Work is currently under way to address that problem and it will be presented in a later paper by Balsara.

2.2. *A Variant of the Basic Algorithm with Upwinding at Magnetosonic Shocks*

In the previous subsection we designed an algorithm that uses the upwinded fluxes that arise from a higher order Godunov scheme to produce a scheme that preserves the divergence-free aspect of the magnetic field to machine accuracy. The scheme used higher order Godunov fluxes that were upwinded on a dimension by dimension basis. If one wishes to design an algorithm that uses just the basic higher order Godunov methodology then that seems to be the best one can do. However, there have been several efforts in the literature to make a multidimensional representation of the wave fields in order to arrive at schemes that are upwinded in a multidimensional fashion. One possible line of development that allows one to introduce multidimensional aspects to the numerical scheme was laid out by Roe [23]. Roe's method consists of extending the concept of the linearized Riemann solver so that multidimensional features in the flow can be selectively projected onto a multiplicity of right eigenvectors. The choice of waves to project is non-unique and has to be made anew when either the dimensionality of the problem is changed or a new hyperbolic system is analyzed. In this paper our goal is to design an algorithm that operates without significant modification in one, two, or three dimensions. For this reason we do not pursue the above-mentioned line of development here. An alternative line of development was explored in the papers by Davis [24], Levy, Powell, and vanLeer [25], LeVeque and Walder [26], and Rumsey, vanLeer, and Roe [27]. That effort consisted of analyzing local features in the flow and rotating the Riemann solver so that the numerical dissipation is maximal in the upwind direction and minimal in the cross-wind direction. This was done by relinquishing the use of the upwinded Godunov fluxes in the cross-wind direction. The fact that these methods try to minimize the cross-wind dissipation by relinquishing the use of the upwinded Godunov fluxes in that direction makes these methods very accurate in several circumstances but

introduces a slight instability in some circumstances. For this reason we retain the use of the higher order Godunov fluxes that are upwinded on a dimension by dimension basis in the work reported here. However, there is an essential idea that emerges from such methods. It consists of making the evaluation of the fluxes (and in our case the electric fields) dependent on the multidimensional features in the flow. This essential idea is very helpful in making an evaluation of the electric field at the zone edges that is upwinded in a multidimensional sense. We motivate the issues in the ensuing paragraph. We then present in the present subsection a variant of the basic algorithm that was presented in the previous subsection. This variant of the basic algorithm allows us to use the fluxes from the basic higher order Godunov scheme in a multidimensional fashion to obtain the electric fields at the zone edges. This variant is more difficult to code. Also, numerical tests, all of which have been based on moving shocks, have shown that it produces results that are practially identical to those produced by the basic algorithm in the previous subsection. It will, however, provide more robustness in simulations where there are standing magnetosonic shocks that are aligned with the grid lines. Thus the use of the variant presented here might be deemed optional in certain simulations but essential in others and it is for this reason that we present it as a variant of the algorithm described in the previous subsection.

To motivate the need for incorporating multidimensional effects consider a situation where a magnetosonic shock was moving along the the x-axis. Then instead of Eq. (9) for the z-component of the electric field a form that has better upwinding in the vicinity of the shock would be

$$E^{n+1/2}_{z,\,i+1/2,\,j+1/2,k} = \tfrac{1}{2}\big(-F^{n+1/2}_{7,\,i+1/2,\,j,k} - F^{n+1/2}_{7,\,i+1/2,\,j+1,k}\big). \tag{17}$$

On the other hand, consider a situation where a magnetosonic shock was moving along the y-axis. Instead of Eq. (9) for the z-component of the electric field a form with better upwinding in the vicinity of the shock would then be given by

$$E^{n+1/2}_{z,\,i+1/2,\,j+1/2,k} = \tfrac{1}{2}\big(G^{n+1/2}_{6,\,i,\,j+1/2,k} + G^{n+1/2}_{6,\,i+1,\,j+1/2,k}\big). \tag{18}$$

If, on the other hand, the flow were locally smooth, Eq. (9) would give the best phase accuracy for the propagation of smooth features in the flow. Thus when discontinuities are present it may be beneficial to allow the evaluation of the electric field to locally adjust to those discontinuities. We point out that the fluxes to be used on the right hand sides of Eqs. (9), (17), and (18) are the higher order Godunov fluxes that have been upwinded on a dimension by dimension basis. Notice too that the evaluation of the z-component of the electric field depends on the orientation of discontinuities in the xy-plane. More generally, the evaluation of the electric field component along a given grid-aligned direction depends on the orientation of discontinuities in the plane that is perpendicular to that direction. Thus we need automated ways for identifying two things. First, we need to be able to confirm that we have a substantially strong discontinuity that lies in the plane that is perpendicular to the direction along which we want to evaluate the electric field. Second, we need to be able to identify the direction of propagation of the discontinuity in that plane. The work of Rumsey, vanLeer, and Roe [27] has shown that it is not advantageous to allow the direction of upwinding to rotate in response to every mild feature in the flow. Thus we want to design switches which identify situations when a shock with a non-trivial shock strength is present in a local region of the flow. Weak shocks are naturally smeared out over several zones by

most higher order Godunov schemes and for such situations Eq. (9) is adequate. It must also be pointed out that one might even require that a similar upwinding be attempted for entropy pulses and torsional Alfvén discontinuities. However, the work of Quirk [28] has shown that higher order Godunov schemes are most suceptible to instabilities when shocks that are aligned with the computational grid propagate slowly across the grid. The same suceptibility to instabilities does not extend to linearly degenerate waves which are not self-steepening. Entropy waves and torsional Alfvén waves are not self-steepening and are smeared over a few zones by all schemes. Thus Eq. (9) should work well in such situations and we do not design a multidimensional upwinding strategy that focusses on the propagation of entropy pulses and torsional Alfvén discontinuities.

In what follows we describe the variant of the basic algorithm for orthogonal grids. In order to give a detailed description, we specialize to the case of evaluating the z-component of the electric field. Thus we design switches that pick out the existence of magnetosonic shocks of non-trivial strength in the xy-plane. It is trivial to repeat the exercise for the other two components of the electric field and in order to save space we do not do that here. The extension to non-orthogonal coordinate systems can be made rather trivially by focussing on the variations in the flow in a plane that is locally perpendicular to the direction along which we want to evaluate the component of the electric field. The first switch is designed to pick out situations where we are in the vicinity of a strong magnetosonic shock or a flow configuration that might develop into such a shock. This is accomplished by taking the L_1 norm of the undivided gradient of the pressure and comparing it with the minimum pressure in the local vicinity. Thus our first switch, **SW1**, is switched on if

$$|\Delta P|_{x,\,i+1/2,\,j+1/2,k} + |\Delta P|_{y,\,i+1/2,\,j+1/2,k} > \tilde{\beta}\,\min(P_{i,\,j,k},\, P_{i+1,\,j,k},\, P_{i,\,j+1,k},\, P_{i+1,\,j+1,k}) \tag{19}$$

and is switched off otherwise. Here we have used $\tilde{\beta} = 0.5$. The method should also pick out strongly compressive motions. A measure of this can be obtained by comparing the undivided divergence of the velocity to the smallest local signal speed. Thus we have our second switch, **SW2**, which is switched on if

$$-\delta\,\min(C_{i,\,j,k},\, C_{i+1,\,j,k},\, C_{i,\,j+1,k},\, C_{i+1,\,j+1,k}) > (\boldsymbol{\nabla}\cdot\mathbf{v})_{xy,\,i+1/2,\,j+1/2,k} \tag{20}$$

and is switched off otherwise. Here we used $\delta = 0.1$. The scheme presented here is in fact rather insensitive to the specific values of $\tilde{\beta}$ and δ and the values can be selected within a reasonable range so that the scheme picks out shocks that are stronger than a specified strength. We have the following auxiliary definitions:

$$|\Delta P|_{x,\,i+1/2,\,j+1/2,k} = \tfrac{1}{2}|P_{i+1,\,j+1,k} + P_{i+1,\,j,k} - P_{i,\,j+1,k} - P_{i,\,j,k}| \tag{21}$$

$$|\Delta P|_{y,\,i+1/2,\,j+1/2,k} = \tfrac{1}{2}|P_{i+1,\,j+1,k} + P_{i,\,j+1,k} - P_{i+1,\,j,k} - P_{i,\,j,k}| \tag{22}$$

$$\begin{aligned}(\boldsymbol{\nabla}\cdot\mathbf{v})_{xy,\,i+1/2,\,j+1/2,k} = {} & \tfrac{1}{2}(v_{x\,i+1,\,j+1,k} + v_{x\,i+1,\,j,k} - v_{x\,i,\,j+1,k} - v_{x\,i,\,j,k}) \\ & + \tfrac{1}{2}(v_{y\,i+1,\,j+1,k} + v_{y\,i,\,j+1,k} - v_{y\,i+1,\,j,k} - v_{y\,i,\,j,k})\end{aligned} \tag{23}$$

$$C_{i,\,j,k} = \left(\frac{\gamma\,P_{i,\,j,k}}{\rho_{i,\,j,k}} + \frac{B^2_{i,\,j,k}}{4\pi\rho_{i,\,j,k}}\right)^{1/2}. \tag{24}$$

When **SW1** and **SW2** are both switched on it means that the flow in a local region has a shock in it. In that case we need to pick out the direction along which we want to upwind the

evaluation of the electric field. We do that by setting the ratio $\psi_{xy,\,i+1/2,\,j+1/2,k}$ defined to be

$$\psi_{xy,\,i+1/2,\,j+1/2,k} = \frac{|\Delta P|_{x,\,i+1/2,\,j+1/2,k}}{|\Delta P|_{x,\,i+1/2,\,j+1/2,k} + |\Delta P|_{y,\,i+1/2,\,j+1/2,k}}. \tag{25}$$

In all other cases we set $\psi_{xy,\,i+1/2,\,j+1/2,k}$ to its default value of $\psi_{xy,\,i+1/2,\,j+1/2,k} = \frac{1}{2}$.

The z-component of the electric field, $E^{n+1/2}_{z,\,i+1/2,\,j+1/2,k}$, can now be written as

$$\begin{aligned} E^{n+1/2}_{z,\,i+1/2,\,j+1/2,k} = {} & \frac{\psi_{xy,\,i+1/2,\,j+1/2,k}}{2}\left(-F^{n+1/2}_{7,\,i+1/2,\,j,k} - F^{n+1/2}_{7,\,i+1/2,\,j+1,k}\right) \\ & + \frac{1-\psi_{xy,\,i+1/2,\,j+1/2,k}}{2}\left(G^{n+1/2}_{6,\,i,\,j+1/2,k} + G^{n+1/2}_{6,\,i+1,\,j+1/2,k}\right). \end{aligned} \tag{26}$$

It is easy to see from Eq. (26) that when the default value of $\psi_{xy,\,i+1/2,\,j+1/2,k}$ is used Eq. (26) is identical to Eq. (9). When the flow has a shock in the vicinity of the zone edge where the z-component of the electric field is being evaluated Eq. (26) picks up contributions from the x-directional and y-directional fluxes that are proportional to the components of the local gradient of the pressure in the xy-plane. Since the local gradient of the pressure is aligned with the direction of propagation of the shock front Eq. (26) always picks out the properly upwinded direction. As a trivial consistency check it is easy to verify that when the shock is propagating along the x-axis Eq. (26) reduces to Eq. (17). Likewise, when the shock is propagating along the y-axis Eq. (26) reduces to Eq. (18). Thus we have designed a strategy that provides the correct multidimensional upwinding in regions which have magnetosonic shocks of non-trivial strength and reduces to Eq. (9) in all other situations.

3. NUMERICAL RESULTS

3.1. *Test Problem 1: The Rotor Problem*

Our first test problem consists of testing the propagation of strong torsional Alfvén waves. It was suggested by Brackbill [29] and is patterned after the problem of angular momentum loss through torsional Alfvén waves in star formation (see Mouschovias and Paleologou [30]). The problem consists of having a dense, rapidly spinning cylinder (the rotor) in a light fluid (the ambient fluid). Here the ambient fluid refers to the rest of the computational domain that excludes the region initially occupied by the rotor. To further clarify the nomenclature, we mention that apart from giving the rotor an initial spin no external body forces are applied to the rotor. The two fluids are threaded by a magnetic field that is uniform to begin with. The rapidly spinning rotor causes torsional Alfvén waves to be launched into the ambient fluid. As a result the angular momentum of the rotor is diminished. The magnetic field is strong enough that as it wraps around the rotor the increased magnetic pressure around the rotor compresses the fluid in the rotor, giving it an oblong shape. The problem is set up on a two dimensional unit square with 400×400 zones. A unit density and pressure are set up in the ambient fluid which is also assumed to be initially static. The rotor is set up in the center of the computational domain. A slight taper is applied to the rotor's density and toroidal velocity to prevent the computation from generating strong start-up transients. Thus the density is set to a value of 10 inside a radius of 0.1. A linear taper is applied to the density so that it drops linearly in the radial variable from a density of 10 at a radius of 0.1 to a density of unity at a radius of 0.115. The taper is, therefore, applied over a distance of six zones in our calculation. The pressure in the rotor is set to the same value as that in the

ambient. The ratio of specific heats was set to 1.4 in both the rotor and the ambient fluid. The rotor rotates with a uniform angular velocity that extends out to a radius of 0.1. At a radius of 0.1 it has a toroidal velocity of two units. Between a radius of 0.1 and a radius of 0.115 the rotor's toroidal velocity drops linearly in the radial variable from two units to zero so that at a radius of 0.115 the velocity blends in with that of the ambient fluid. A magnetic field with an initial magnitude of five units that is initially uniform and oriented along the x-axis is set up over the entire computational domain. As a result the magnetic field threads both the rotor and the ambient fluid, thus allowing angular momentum through torsional Alfvén waves to be communicated from the rotor to the ambient. The magnetic field is given an initial value of five units. The problem was run with a Courant number of 0.8. It was stopped at a time of about 0.295, by which time the torsional Alfvén waves have almost reached the boundary.

Figures 2a–d show contour plots for the density, pressure, Mach number, and magnetic pressure when the problem was run with the scheme described here for maintaining solenoidal magnetic fields. The figure shows the variables at a time of 0.295. The algorithm described in Subsection 2.1 was used. We also used the algorithm described in

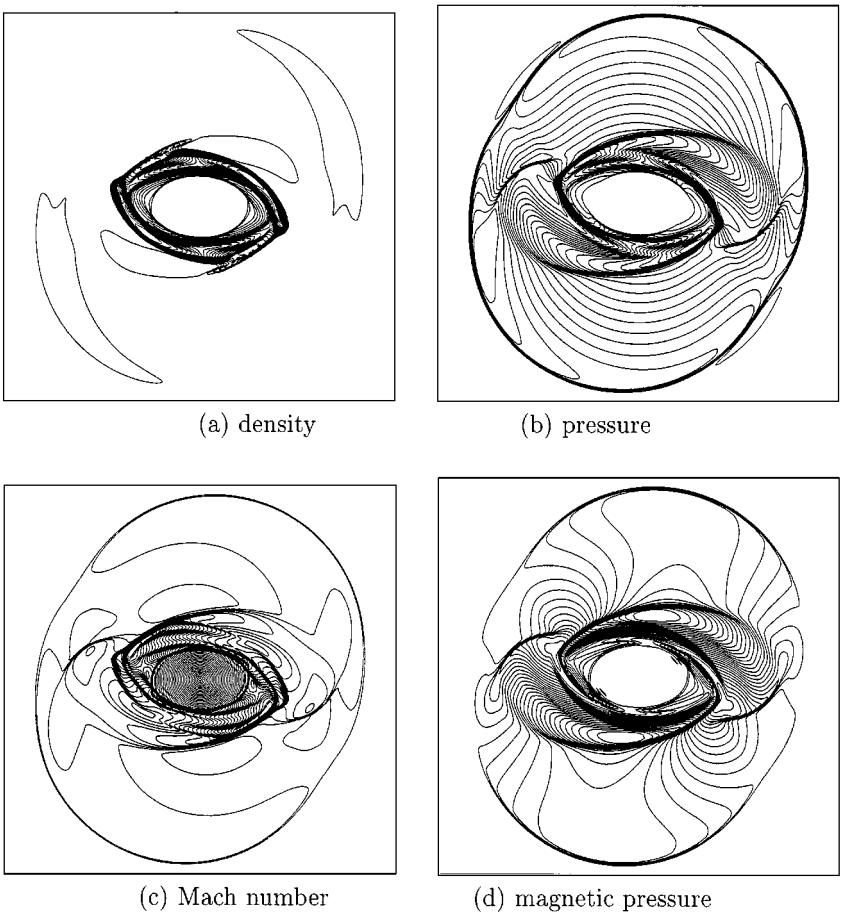

FIG. 2. The results from the rotor test problem described in the text. The results pertain to a simulation time of 0.295 and were run with the divergence-free scheme described in Subsection 2.1.

Subsection 2.2 for this problem and obtained identical results. It is also worth mentioning that the higher order Godunov fluxes used in this and subsequent subsections were obtained by using the TVD scheme for the RIEMANN code described in Balsara [12, 13]. Figures 3a–d show similar variables when the problem was run with a zone centered scheme to which no divergence cleaning was applied. The figure shows the variables at a time of 0.317. Figure 3e shows the ratio of the undivided divergence of the magnetic field to the magnitude of the magnetic field in this problem. From Fig. 2 we observe that the rotor does launch torsional Alfvén waves, as expected. Those Alfvén waves show up very clearly in the plots for the magnetic pressure. It is also possible to see from the density contours that the rapid buildup of magnetic pressure around the rotor's outer boundary causes the fluid in the rotor to be compressed, giving it an oblong shape.

We can see from the Mach number contours that within the rotor the fluid is still in uniform rotation out to a certain radial distance but beyond that distance the toroidal motion of the rotor's fluid has had its angular momentum lowered because it has exchanged angular momentum with the ambient fluid. Thus the numerical scheme presented here is behaving as expected. Figure 3 corresponds to a zone centered scheme to which no divergence cleaning is applied. It corresponds to a time slightly later than that of Fig 2. Even though the tip of the outward-going Alfvén wave has gone off the computational domain we have picked that time step because it shows the consequences of allowing the buildup of divergence in a very dramatic fashion. Had we displayed Fig. 3 at a time that is comparable to the time of Fig. 2 it would still have shown the deleterious effects of allowing a non-zero divergence to build up in the magnetic field though in not quite such a dramatic fashion. We see from the plots of the density, Mach number, and magnetic pressure that the region on the boundary and in the interior of the rotor has been corrupted by a spurious solution. We also ran the same zone centered calculation with a divergence cleaning step and found that it looks just like Fig. 2. This gives us reason to believe that it is the lack of divergence cleaning that causes the growth of the spurious solution in Fig. 3. In this problem we expect the magnetic field lines to be maximally sheared at the boundary between the rotor and the ambient fluid. Thus we expect that the errors will build up fastest in that region. As a result we expect magnetic monopoles to form there. The fact that the spurious solution has grown exactly in that local region gives us reason to believe that the buildup of magnetic monopoles has caused the spurious dynamics to develop in that region. Figure 3e shows one possible measure of the strength of magnetic monopoles. The minimum and maximum in that figure go from -0.66 to 0.66. This shows that the buildup of the unphysical, i.e., compressive, part of the magnetic field is significant and comparable in magnitude to the magnetic field itself. It helps to bear out our contention that the buildup in a local region over long periods of simulation time of the inevitable discretization errors that would have arisen in any numerical scheme has caused strong magnetic monopoles to develop. We also point out that our resolution of 400×400 zones would be considered high enough for this class of problem. Thus increasing the resolution will not prevent the magnetic monopoles from forming.

In Balsara [12, 13] we showed that a similar buildup of locally strong magnetic monopoles can take place in the Orzag–Tang test problem if it is run long enough. We showed in that paper that divergence cleaning could solve the problem. We were able to run the same problem with the method given here and have obtained results that are comparable in quality to the simulations where a divergence cleaning is applied. Because the late time evolution of the Orzag–Tang test problem is thoroughly catalogued in Balsara [12, 13] we do not repeat the solutions here.

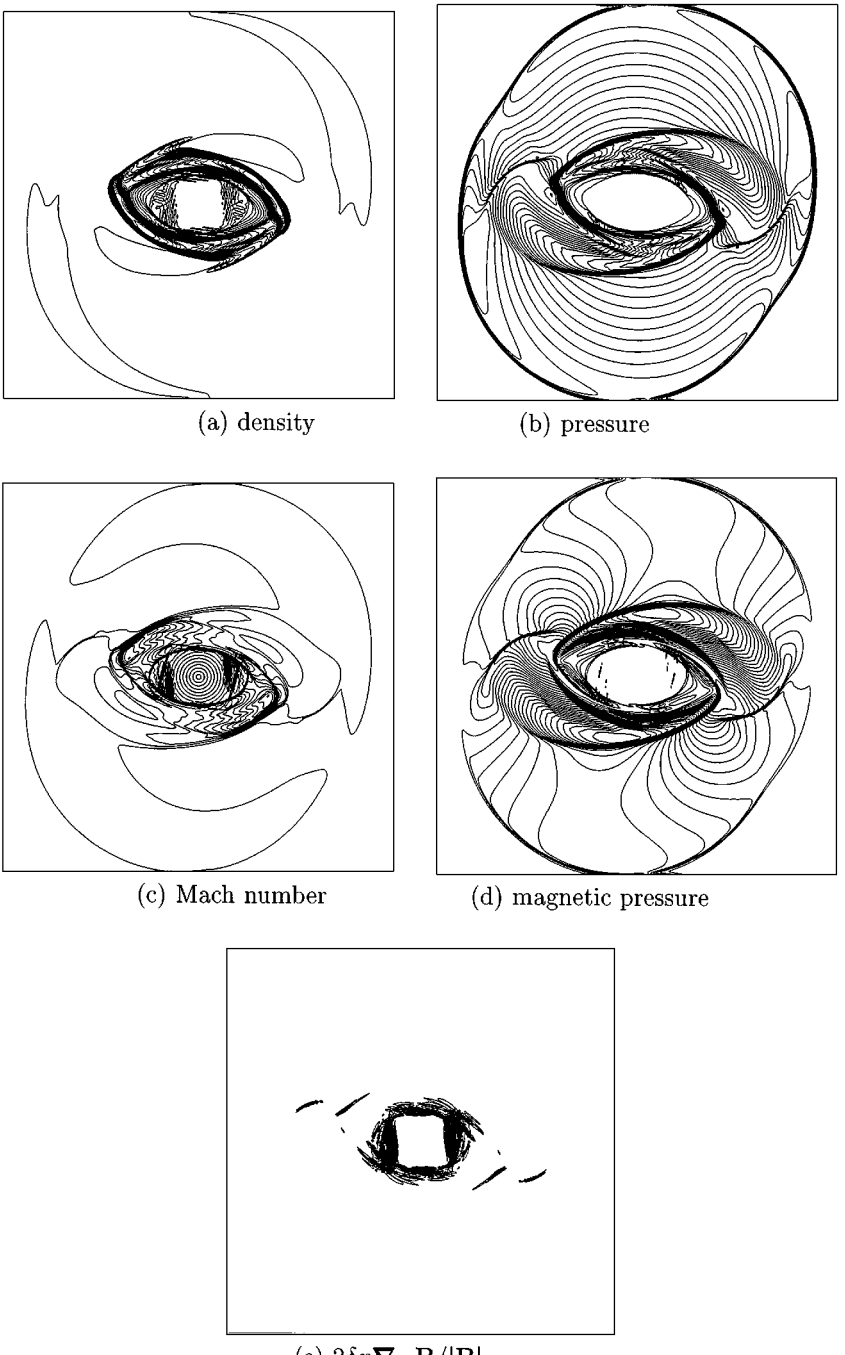

FIG. 3. The results from the rotor test problem described in the text. The results pertain to a simulation time of 0.317 and were run with the a zone centered higher order Godunov scheme without any divergence cleaning.

3.2. *Test Problem 2: The Blast Problem*

Our scheme involves a staggered collocation of magnetic field components. It has long been believed in the fluid dynamics community that schemes that use staggered collocations of field variables are not as robust as zone centered schemes, especially in the vicinity of shocks. However, that body of experience has been built up solely on the basis of schemes that utilize artificial viscosity formulations in order to handle shocks. Higher order Godunov schemes have always been formulated as zone centered schemes. In fact it is so natural to formulate them in that fashion that there has been no impetus so far to understand their behavior when a staggered collocation of variables is used. As a result there has not been a body of experience built up so far on how a scheme with a staggered collocation of variables would perform when properly upwinded and consistent higher order Godunov fluxes are used in the time update. The results of the test problem of the previous subsection give us some confidence that a scheme which uses a staggered collocation along with properly upwinded higher order Godunov fluxes does indeed perform well and yields results that are competitive with zone centered formulations. But none of the problems presented so far involved very strong magnetosonic shocks in multiple dimensions. Thus we have constructed a problem involving a strong blast wave. This is a more stringent variant of the problem presented in Balsara [12, 13]. The problem is again set up on a unit square with 200×200 zones. The initial density is set to unity all over. The initial pressure is set to 0.1 all over except in a central circle of radius 0.1 where it is set to 1000. The ratio of specific heats was 1.4. The initial velocity is zero. A magnetic field with a magnitude of 100 is initialized along the x-direction. Thus the fluid in the region outside the initial pressure pulse has a very small plasma β. Figures 4a–d show the density, pressure, square of the total velocity, and magnetic pressure. The algorithm described in Subsection 2.1 was used. We ran the same problem with a zone centered higher order Godunov scheme with divergence cleaning and found results that are extraordinarily similar. This shows that our scheme, despite its use of a face centered collocation for the magnetic field variables, performs robustly and accurately even in the regime of strong shocks. To further explore the role of multidimensional effects emerging from the propagation of strong shocks we ran the same test problem with the algorithm described in Subsection 2.2 and found results that were identical to those shown in Fig 4. To further explore the nature of the staggered mesh algorithm presented here we also ran the test problem with $\psi_{xy,\, i+1/2,\, j+1/2,k} = 1$ in Eq. (26), so that Eq. (26) actually reduced to Eq. (17) at all zone edges, and found only the slightest degradation in the propagation of shocks in the z-direction. We also ran the same test problem with $\psi_{xy,\, i+1/2,\, j+1/2,k} = 0$ in Eq. (26) and found only the slightest degradation in the propagation of shocks in the x-direction. Thus the staggered mesh algorithm presented here seems to perform robustly and is not strongly dependent on the multidimensional effects that are incorporated in the evaluation of the electric fields. The natural explanation for this robust and accurate performance is that we use consistent and properly upwinded higher order Godunov fluxes in the evaluation of the electric fields.

We also ran the blast problem with a zone centered higher order Godunov scheme without divergence cleaning. The results look very similar to Fig. 4. As a general rule we have found that strong shocks moving rapidly with respect to the computational mesh do not produce situations where the effect of having magnetic monopoles in the calculation stands out prominently. To really see the damaging consequences of having magnetic monopoles in the calculation one should do problems like the rotor problem above or problems involving stationary shocks where the errors have a long time to build up in local regions of the flow.

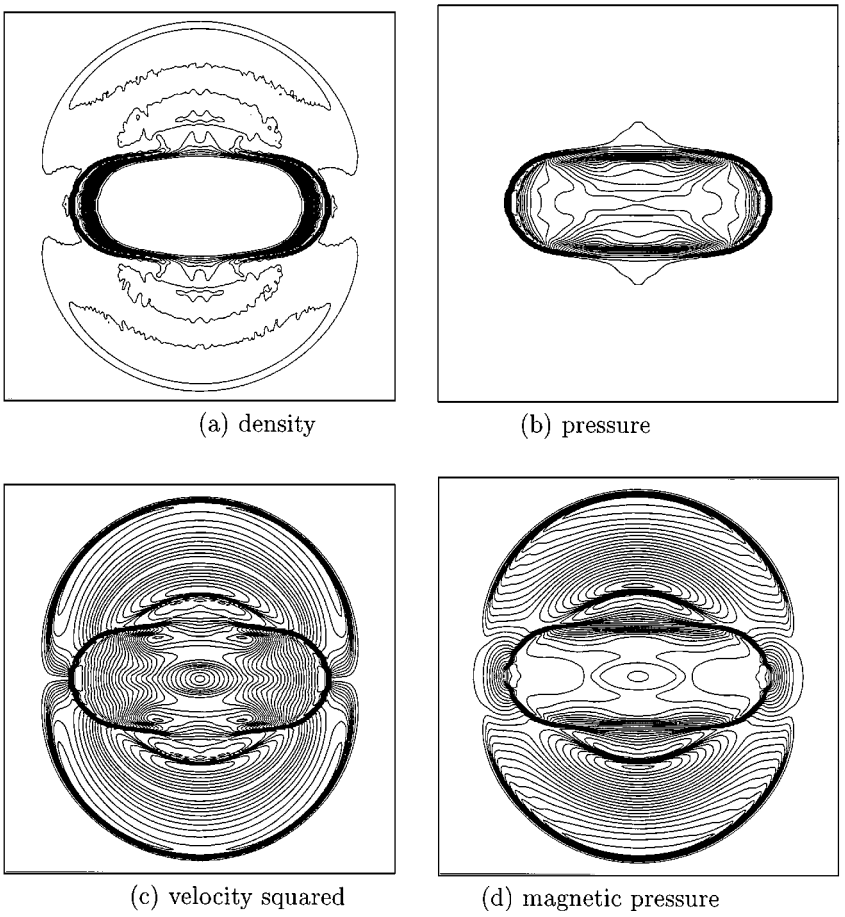

FIG. 4. The results from the blast problem described in the text. The results pertain to a simulation time of 0.01 and were run with the divergence-free scheme described in Subsection 2.1.

3.3. *Test Problem 3: The Oblique Propagation of Alfvén Waves*

Our last test problem was suggested by D. Barnes [31]. It consists of realizing that when Alfvén or slow waves propagate nearly orthogonal to the direction of the magnetic field their propagation speeds become very small and comparable to each other. The fact that the speeds of the two families of waves are comparable implies that small discretization errors made in the propagation of one wave family will excite oscillations in the other wave family. Thus the propagation of Alfvén waves in directions that are almost orthogonal to the direction of the magnetic field has been known to be a challenging problem for several numerical MHD codes. Unfortunately, this is also an important issue in several numerical applications. A good example would be numerical simulation of MHD turbulence. The theory (see Kraichnan [32]) requires that the wave modes that interact with each other form closed triangles. But if certain wave modes cannot propagate with fidelity in a given numerical code then those modes will not be represented in the formation of a turbulent spectrum. This becomes an especially severe problem since such simulations are bound by the resolution available on parallel supercomputers and an ability to capture wave modes with some level of fidelity with the smallest possible number of zones translates into an advantage.

Even from a numerical point of view it may be argued that since the present method utilizes staggered collocation for the magnetic fields it may change the wave propagation characteristics. As a result we perform a multiresolution study using 30×30, 60×60, and 120×120 zones on the two dimensional domain, taken to be the x,y-plane, given by $[0.0, 6.0] \times [0.0, 6.0]$.

The density is set to unity, as is the pressure. The ratio of specific heats was 1.4. The unperturbed velocity in the fluid is set to zero. An unperturbed unit magnetic field is initialized in the x-direction. An Alfvén wave with a wavelength of $6/\sqrt{37}$ is initialized so that it propagates at an angle of $\tan^{-1}(6) = 80.5376$ degrees to the magnetic field within the x,y-plane constituted by the computational domain. The Alfvén wave, therefore, travels with a speed given by $V_A = 0.046376$. Thus while there are 30, 60, and 120 zones to represent the wave in the y-direction in the three simulations in this multiresolution study, there are only 5, 10, and 20 zones in the simulations to represent the wave in the x-direction. The very small number of zones available in the x-direction to capture the x-directional wave-number of the Alfvén wave is what makes this a stringent test problem. In order to set up an Alfvén wave we have to apply fluctuations to the z-velocity and z-component of the magnetic field. The problem is so initialized that the amplitude of the z-velocity is given by 0.2 initially. The amplitude of the z-component of the magnetic field is $0.2\sqrt{4\pi}$. It must be pointed out that this multidimensional problem has an exact analytical solution. The analytical expressions for the perturbed z-velocity and z-component of the magnetic field can be given at the initial time, and in fact for all later times, by the formulae

$$\phi = \frac{2\pi\sqrt{37}}{6}\left(\frac{1}{\sqrt{37}}x + \frac{6}{\sqrt{37}}y - V_A t\right) + \phi_o \tag{27}$$

$$v_z = 0.2\cos\phi \tag{28}$$

$$B_z = -0.2\sqrt{4\pi}\cos\phi. \tag{29}$$

Here ϕ_o is an arbitrary constant. Periodic boundary conditions are applied in the x- and y-directions. It must be pointed out that the region of interest is just the region $[0.0, 6.0] \times [0.0, 1.0]$, which contains one complete cyclic period of the wave. But doing the problem in that region would have required using somewhat complicated boundary conditions. As a result, we choose a computational domain that is six times larger so that the phases from Eq. (27) for the lower y-boundary and the upper y-boundary match exactly. This simplifies the boundary conditions and allows us to use the periodic boundary conditions, which are far simpler to implement. The problem is run with a Courant number of 0.8 for a simulation time given by 131.161. This time corresponds to one entire traversal of the Alfvén wave from the origin to the point (1, 6).

Figure 5a shows the z-velocity on the first row of $y =$ constant zones at the last time step in the simulation. The legends 0, 1, and 2 correspond to the simulations using 30×30, 60×60, and 120×120 zones, respectively. An offset of 0.1 was applied in the vertical direction to the legends corresponding to 1 and an offset of 0.2 was applied to the legends corresponding to 2. Figure 5b corresponds to the z-component of the magnetic field. Here the offsets are 0.3 corresponding to legend 1 and 0.6 corresponding to legend 2. Figures 5a and b correspond to the scheme presented in this paper. The scheme described in Subsection 2.1 was used to obtain the results shown in Fig. 5. Figures 6a and b are exactly analogous to Figs. 5a and b with the exception that they were obtained using a zone centered higher order Godunov

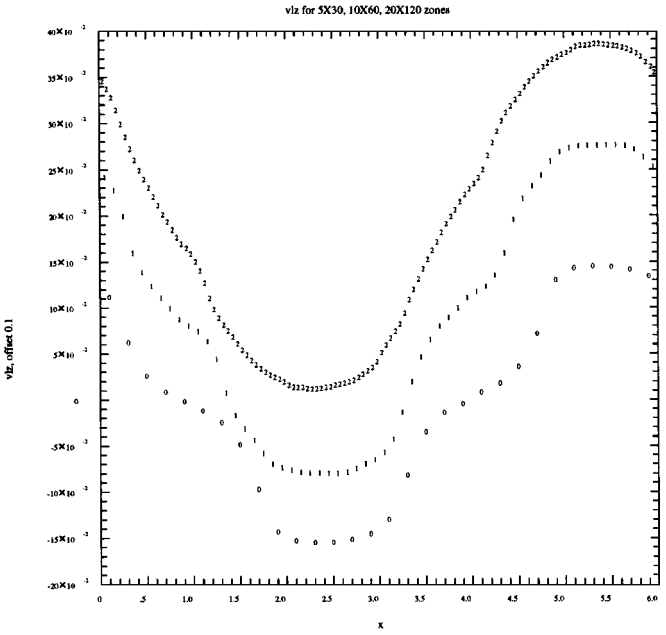

(a) z-velocity

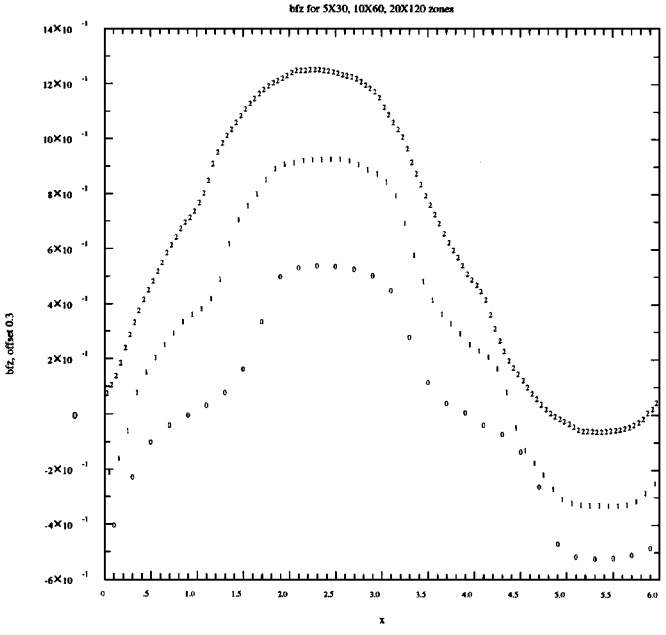

(b) z-component of the magnetic field

FIG. 5. (a) The z-velocity on the first row of $y =$ constant zones at the last time step obtained from the oblique Alfvén wave test problem. The scheme described in Subsection 2.1 was used here. The legends 0, 1, and 2 correspond to the simulations using 30×30, 60×60, and 120×120 zones, respectively. An offset of 0.1 was applied in the vertical direction to the legends corresponding to 1 and an offset of 0.2 was applied to the legends corresponding to 2. (b) The z-component of the magnetic field. Here the offsets are 0.3 corresponding to legend 1 and 0.6 corresponding to legend 2. Parts (a) and (b) correspond to the scheme presented in the paper.

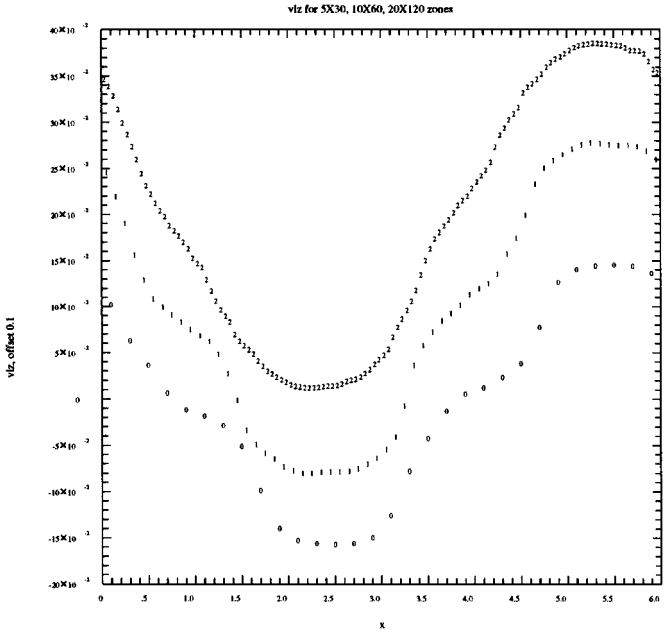

(a) z-velocity

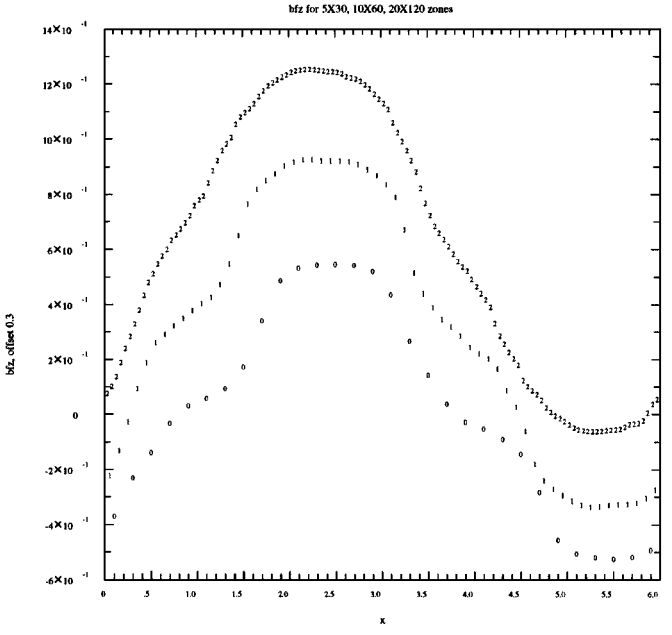

(b) z-component of the magnetic field

FIG. 6. This figure is similar to Figs. 5a and b. The only difference is that this time a zone centered higher order Godunov scheme was used.

scheme. We find that the figures are entirely comparable and Fig. 5 even shows a very slight improvement over Fig. 6 at higher resolutions. Thus we see that the collocation of magnetic fields at face centers has not in any way damaged the wave propagation characteristics of the scheme and may even have improved it very slightly. We also see that when only 5 zones are available to resolve the x-directional wavenumber there is a noticeable decrement in the z-velocity and the z-component of the magnetic field after the wave has traversed the computational domain once. When only 10 zones are available to resolve the x-directional wavenumber the amplitude is properly captured though the phase information is still not properly captured, as shown by the fact that the curves corresponding to legend 1 in either Fig. 5 or Fig. 6 are morphologically quite different from a sinusoid. When 20 zones are available to resolve the x-directional wavenumber we see that the amplitude information is captured very well and the phase information is also properly captured. In all cases the waves were properly propagated as Alfvén waves and the mode mixing with slow magnetosonic waves was held down to the level of discretization error.

4. CONCLUSIONS

In this paper we have developed a scheme that ensures that the magnetic fields in an MHD simulation remain strictly solenoidal up to discretization error. This has been done in the context of higher order Godunov schemes. The scheme requires the components of the magnetic field to be collocated at the face centers. A duality is established between the electric fields and the fluxes that are obtained in a higher order Godunov scheme. This duality is utilized to obtain electric fields at the edges of the computational zones through a reconstruction process that is applied directly to the properly upwinded fluxes that are obtained from the higher order Godunov scheme. The electric fields are then utilized to make an update of the magnetic fields that preserves the solenoidal nature of the magnetic fields. We have even presented a variant of the basic algorithm that utilizes multidimensional features in the flow to select the upwinded direction for the evaluation of the electric fields. It is expected that this variant of the basic algorithm will be very useful in the accurate treatment of strong standing shocks that are aligned with respect to the computational grid. It also provides a very desirable conceptual completeness to the scheme presented here. The scheme described here is general and applies equally well to predictor–corrector and multi-stage time stepping formulations.

The resulting scheme is robust and accurate. In that sense it shares the best properties of the higher order Godunov schemes that were used in its formulation. By comparing its performance with similar schemes where a divergence cleaning step is applied to a straightforward higher order Godunov scheme it is shown that the different collocation that is used here for the magnetic field variables does not produce any degradation of the results. The physical explanation for that stems from the fact that we have built the electric fields directly and consistently from the properly upwinded higher order fluxes themselves. We have shown that this robust performance persists even in the presence of very strong multidimensional magnetosonic shocks. We have also shown that despite the staggered collocation of magnetic field variables the phase accuracy of the scheme is as good as that of a zone centered collocation of variables. It is also useful to point out that in the limit where the magnetic fields are very weak or non-existent the scheme reduces exactly to a traditional higher order Godunov scheme.

We have also shown that in certain circumstances the local buildup of a dynamically significant compressive component in the magnetic field cannot be avoided when neither the scheme presented in this paper nor a divergence cleaning step is used. We have shown that over long integration times this buildup can be substantial. It can, therefore, affect the numerical solution to the point of having the computed solution diverge from the physical solution. It has often been claimed that the much-touted high accuracy of higher order Godunov schemes makes it unnecessary to suppress the divergence of the magnetic field in calculations using such schemes. That much-touted high accuracy has, therefore, been shown to be an inadequate foil against the harmful effects caused by the buildup of divergence in the magnetic fields. As a result a strong case is made in favor of utilizing this scheme (or perhaps a divergence cleaning step) in all MHD simulations that are carried out with higher order Godunov schemes.

ACKNOWLEDGMENTS

This work was supported by the NASA Space Physics Theory Program. One of us (D.B.) also wishes to acknowledge the use of supercomputer time at SDSC and PSC.

REFERENCES

1. J. U. Brackbill and D. C. Barnes, *J. Comput. Phys.* **35**, 462 (1980).
2. J. Brackbill, *Space Sci. Rev.* **42**, 153 (1985).
3. K. S. Yee, Numerical solution of initial boundary value problems involving Maxwell's equations in isotropic media, *IEEE Trans. Antenna Propagation* **AP-14**, 302 (1966).
4. S. H. Brecht, J. G. Lyon, J. A. Fedder, and K. Hain, *Geophys. Res. Lett.* **8**, 397 (1981).
5. C. H. Evans and J. H. Hawley, *Astrophys. J.* **332**, 659 (1989).
6. R. DeVore, *J. Comput. Phys.* **92**, 142 (1991).
7. J. M. Stone and M. L. Norman, *J. Suppl.* **80**, 791 (1992).
8. A. L. Zachary, A. Malagoli, and P. Colella, *SIAM J. Sci. Comput.* **15**, 263 (1994).
9. W. Dai and P. R. Woodward, *J. Comput. Phys.* **115**, 485 (1994).
10. D. Ryu and T. Jones, *Astrophys. J.* **442**, 228 (1995).
11. P. L. Roe and D. S. Balsara, *SIAM J. Appl. Math.* **56**, 57 (1996).
12. D. S. Balsara, *Astrophys. J. Suppl.* **116**, 119 (1998).
13. D. S. Balsara, *Astrophys. J. Suppl.* **116**, 133 (1998).
14. K. Powell, ICASE Report 94-24, Langley, VA (1994).
15. W. L. Dai and P. Woodward, *Astrophys. J.* **494**, 317 (1998).
16. W. E and C. W. Shu, *J. Comput. Phys.* **110**, 39 (1994).
17. J. Bell, P. Colella, and H. Glaz, *J. Comput. Phys.* **85**, 257 (1989).
18. B. van Leer, in *Computing Methods in Applied Science and Engineering IV*, edited by R. Glowinski and J. L. Lions (North-Holland, Amsterdam, 1984), p. 493.
19. P. Colella, *J. Comput Phys.* **87**, 171 (1990).
20. C.-W. Shu and S. Osher, *J. Comput. Phys.* **77**, 439 (1988).
21. A. Harten, B. Engquist, S. Osher, and S. Chakravarthy, *J. Comput. Phys.* **71**, 231 (1987).
22. J. Casper and H. L. Atkins, *J. Comput. Phys.* **106**, 62 (1993).
23. P. L. Roe, *J. Comput. Phys.* **63**, 458 (1986).
24. S. F. Davis, *J. Comput. Phys.* **56**, 65 (1984).

25. D. W. Levy, K. G. Powell, and B. vanLeer, AIAA Paper 89-1931 (1989).
26. R. J. LeVeque and R. Walder, *Notes Numer. Fluid Mech.* **35**, 376 (1991).
27. C. L. Rumsey, B. vanLeer, and P. L. Roe, *J. Comput. Phys.* **105**, 306 (1993).
28. J. Quirk, *Int. J. Numer. Methods Fluids* **18**, 555 (1994).
29. J. U. Brackbill, LANL Workshop on Numerical MHD, 1986.
30. T. Ch. Mouschovias and Paleologou, *Astrophys. J.* **237**, 877 (1980).
31. D. Barnes, Private communication, 1997.
32. R. H. Kraichnan, *Phys. Fluids* **8**, 1385 (1965).